



Heriot-Watt University
Research Gateway

Evolution, the loss of diversity and the role of trade-offs

Citation for published version:

Best, A, Bowers, R & White, A 2015, 'Evolution, the loss of diversity and the role of trade-offs', *Mathematical Biosciences*, vol. 264, no. 1, pp. 86-93. <https://doi.org/10.1016/j.mbs.2015.03.011>

Digital Object Identifier (DOI):

[10.1016/j.mbs.2015.03.011](https://doi.org/10.1016/j.mbs.2015.03.011)

Link:

[Link to publication record in Heriot-Watt Research Portal](#)

Document Version:

Peer reviewed version

Published In:

Mathematical Biosciences

Publisher Rights Statement:

© 2015 Elsevier Inc. All rights reserved.

General rights

Copyright for the publications made accessible via Heriot-Watt Research Portal is retained by the author(s) and / or other copyright owners and it is a condition of accessing these publications that users recognise and abide by the legal requirements associated with these rights.

Take down policy

Heriot-Watt University has made every reasonable effort to ensure that the content in Heriot-Watt Research Portal complies with UK legislation. If you believe that the public display of this file breaches copyright please contact open.access@hw.ac.uk providing details, and we will remove access to the work immediately and investigate your claim.

Evolution, the loss of diversity and the role of trade-offs

by Alex Best^{1*}, Roger Bowers² and Andy White³

Address:

¹School of Mathematics and Statistics University of Sheffield, Sheffield, S3 7RH

²Department of Mathematical Sciences, Mathematical Sciences Building, The University of Liverpool, Liverpool, L69 7ZL, U.K.

³Department of Mathematics and the Maxwell Institute for Mathematical Sciences, Heriot-Watt University, Edinburgh, EH14 4AS, Scotland, UK.

*Corresponding author: a.best@shef.ac.uk

Running Head: Trade-offs and the loss of diversity

Keywords: trade-offs, life history evolution, adaptive dynamics, host resistance, trait extinction

Abstract: We investigate how the loss of previously evolved diversity in host resistance to disease is dependent on the complexity of the underlying evolutionary trade-off. Working within the adaptive dynamics framework, using graphical tools (pairwise invasion plots, PIPs; trait evolution plots, TEPs) and algebraic analysis we consider polynomial trade-offs of increasing degree. Our focus is on the evolutionary trajectory of the dimorphic population after it has been attracted to an evolutionary branching point. We show that for sufficiently complex trade-offs (here, polynomials of degree three or higher) the resulting invasion boundaries can form closed 'oval' areas of invadability and strategy coexistence. If no attracting singular strategies exist within this region, then the population is destined to evolve outside of the region of coexistence, resulting in the loss of one strain. In particular, the loss of diversity in this model always occurs in such a way that the remaining strain is not attracted back to the branching point but to an extreme of the trade-off, meaning the diversity is lost forever. We also show similar results for a non-polynomial but complex trade-off, and for a different eco-evolutionary model. Our work further highlights the importance of trade-offs to evolutionary behaviour.

Introduction

The aim of this paper is to investigate the role that trade-offs between beneficial mutations and fitness costs play in determining evolutionary outcomes, particularly the loss of diversity. Our focus is on the problem of how complex a trade-off must be in order for previously evolved dimorphism to be subject to evolutionary loss. Our study is undertaken in the context of the evolution of host resistance to micro-parasitism (but we expect our key findings to apply more generally).

In common with much contemporary work in evolutionary ecology our investigation is conducted within the framework of adaptive dynamics (Metz et al. 1996; Geritz et al. 1998), which allows the study of trait substitution sequences resulting from the challenge of a resident strain by a closely similar mutant. In particular, we use PIPs (pairwise invadability plots) and TEPs (trait evolution plots), and augment these with numerical simulation of the evolutionary process. Our focus on trade-offs reflects the widely recognised view in life-history theory that they are critical in determining evolutionary behaviour (see Stearns, 1992; Roff, 2002 for reviews). Moreover, there is experimental support for their importance in the evolution of host resistance in particular (Boots and Begon 1993, Kraaijeveld and Godfray 1997, Mealor and Boots 2006). Our concern with the complexity (algebraic, geometric) of the trade-off reflects the finding that the shape of these functions is crucial to the outcomes in a range of ecological systems and is central to much of adaptive dynamics theory (de Mazancourt and Dieckmann 2004; Rueffler et al. 2004; Bowers et al. 2005). Naively, we may expect that increasing the complexity of the trade-off may lead to a more complex outcome; certainly we might expect more local evolutionary niches to exist along the trade-off curve and therefore an increase in diversity. Here, however, we shall show the opposite; that a more complex trade-off causes a reduction in diversity as evolutionary branches are driven to extinction.

Other adaptive dynamics studies have addressed the question of the extinction of evolutionary branches in which the evolutionary trajectory of coexisting strategies leads out of the domain of trait values where those strategies are able to coexist (Kisdi et al 2001). This may lead to branching-extinction cycles, whereby following evolutionary branching one of the coexisting strategies becomes extinct and the other evolves back to the branching point (and the cycle repeats) (Kisdi et al 2001, Dercole 2003) or to a monomorphic population following the extinction of one of the strategies (e.g. Geritz, et

al., 1999; Kisdi 1999). The extinction of evolutionary branches (and particularly branching-extinction evolutionary cycles) has also been observed in stochastic simulation models that represent a range of ecological systems/scenarios (Van der Laan and Hogeweg 1995; Doebeli and Ruxton 1997; Koella and Doebeli 1999; Doebeli and Dieckmann 2000; Johansson et al 2010; Ammutet et al 2014). Our approach differs from previous studies in that we explicitly focus on the role of trade-offs in the extinction of evolutionary branches.

To make our investigation concrete we concentrate on a system for which the application of the method of trade-off and invasion plots (TIPs) (Bowers et al., 2005, Bowers, 2011) has allowed certain properties to be firmly established (Hoyle et al., 2008), namely the evolution of host resistance to parasitism. In this system, when host defence comes at accelerating costs (each additional unit of benefit is met by an increased cost) an evolutionary singularity is both evolutionarily stable (ES) and convergent stable (CS) and hence is an attractor or continuously stable strategy; when this trade-off is sufficiently strongly decelerating it is neither ES nor CS and hence an evolutionary repeller; when the trade-off is sufficiently weakly decelerating it is not ES but is CS and hence a branching point. In this last case, diversity evolves since close to the singularity an initial monomorphic population splits into two coexisting strains and becomes dimorphic. These results are local and determine behaviour near a singularity. To investigate what happens globally – and in particular whether diversity can be lost – we turn to the algebraic presentation of adaptive dynamics and the representation in terms of Pairwise Invadability Plots (PIPs) and Trait Evolution Plots (TEPs) (see Metz et al 1996; Geritz et al 1998). This has the advantage of showing a global picture of invasion boundaries (which separate regions where a resident strain can and cannot be invaded by any mutant) and of associated evolutionary singularities. What is lost in the presentation of any one PIP/TEP is the ability to discuss the effect of varying the trade-off. However, for the present purposes this is manageable as we are interested in whether dimorphic orbits emerging from branching points can subsequently cross boundaries of regions of mutual invadability/strain coexistence. We can investigate this algebraically without specifying the precise trade-off but only its ‘complexity’ – for example its polynomial degree. Using explicit trade-offs, this can be then be illustrated with PIPs/TEPs and we highlight the evolutionary behaviour using simulations of the adaptive dynamics process.

In the next section, we introduce our model and present an analysis for polynomial trade-offs of increasing degree. We undertake algebraic analysis and illustrate our results using

PIPs and TEPs. In particular, the TEPs display regions of mutual invadability/coexistence via the overlap of a PIP and its reflection in the graph of the identity function. Furthermore, they show representative dimorphic orbits obtained from the solution of the canonical equation (Dieckmann & Law, 1996). In our use of TEPs we focus on the region in the upper part of the plane. Our plots relate to numerical examples and are augmented by simulations of the evolutionary process, presented as strain or coexisting strains vs time (using methods in e.g. Boots et al 2014). It transpires that the number of simultaneous branches of the invasion boundary on the PIP is pivotal, in particular, via the possibility that these enclose 'oval' areas of invadability and potentially distinct, enclosed, regions of strategy coexistence on the TEP. When such oval areas occur, in the absence of a co-singular attractor, the evolutionary orbit emanating from a branching point is destined to cross a boundary of mutual invadability causing evolutionary loss of evolved diversity. The question we address is how does the occurrence of such behaviour depend on the complexity of the trade-off.

The Model and its Analysis

We focus our investigations on a model (Hoyle et al., 2008) of hosts evolving resistance to infection (but show that our results also apply to a predator-prey system in Appendix 2). In particular we use an SIS (susceptible-infected-susceptible) framework, with the dynamics of susceptible, X , and infected, Y , hosts as follows

$$\begin{aligned} dX / dt &= aX - qX(X + Y) - bX - sXY + xY \\ dY / dt &= sXY - (r + b + x)Y \end{aligned} \tag{1}$$

Hosts are born susceptible at rate a , which is reduced due to crowding by $q(X + Y)$ (infected hosts do not reproduce). All hosts suffer background mortality at rate b . Disease transmission is modelled by a mass action term between susceptible and infected hosts with transmission coefficient s . Infected hosts suffer additional mortality at rate r (virulence) and recover to susceptibility at rate x .

We assume a mutant strain, with parameters a' and s' , emerges at low density in an environment set by the resident, with stable equilibrium (X^*, Y^*) of equation (1) (see Appendix 1). A proxy for the invasion fitness is (see Appendix 1)

$$s(b, b') = (a + b + g)(a' - q(X^* + Y^*) - b - b'Y^*) + gb'Y^* \quad (2)$$

the notation anticipates the introduction of a trade-off $a = f(s)$. To simplify the algebra in a way which does not affect the general argument we take $q = b = x = r = 1$. This gives

$$s(s, s') = 3a' - 9 \frac{(as + s)}{s(2s + 3)} - 3 - \frac{6s'(as - s - 3)}{s(2s + 3)}. \quad (3)$$

It follows that the fitness is zero when

$$6s(-a's + s'a) + 18(s - s') + 9s(a - a') + 6s(s - s') = 0 \quad (4)$$

which, as must be the case, is satisfied when the two strains are identical.

Our aim in this paper is to reveal the role that the complexity of the trade-off plays in determining aspects of the evolutionary behaviour. We shall discuss polynomial trade-offs of increasing degree (although see a sinusoidal example in Appendix 2) and largely - though not exclusively - concentrate on evolutionary behaviour leading to the loss of previously evolved diversity. As argued above closed regions (ovals) on the PIP are implicated in such behaviour.

We first briefly summarise the known behaviour of this model for a monomorphic host population. From (2) it is easy to show that an evolutionary singular point occurs when

$$\left. \frac{\partial s}{\partial b'} \right|_{b'=b} = 0 \Rightarrow \frac{da}{db} = \frac{(a + b)Y^*}{(a + b + g)}$$

Given this condition, the evolutionary (ES) and convergence (CS) stability properties at this point are

$$\text{ES: } \left. \frac{\partial^2 s}{\partial b^2} \right|_{b'=b} = \frac{d^2 a}{db^2} (a + b + g) < 0$$

$$\text{CS: } \left. \frac{\partial^2 s}{\partial b^2} \right|_{b'=b} + \left. \frac{\partial^2 s}{\partial b \partial b} \right|_{b'=b} = \frac{d^2 a}{db^2} (a + b + g) - \frac{q(a + b)(a + b + g)^2}{b^2 [q(a + b + g) + b(a + b)]} < 0$$

The following outcomes at the singular point are therefore possible:

- If $\frac{d^2 a}{db^2} < 0$, the singular point is both ES and CS and the point is an attractor;
- If $0 < \frac{d^2 a}{db^2} < \frac{q(a + b)(a + b + g)}{b^2 [q(a + b + g) + b(a + b)]}$, the singular point is CS but not ES and so is an evolutionary branching point, causing the generation of two coexisting strains;
- If $\frac{d^2 a}{db^2} > \frac{q(a + b)(a + b + g)}{b^2 [q(a + b + g) + b(a + b)]}$, the singular point is neither ES nor CS and so is a repeller, and the population will evolve to either an extreme of evolution or another singular point.

In particular we note the importance of the trade-off curvature, $d^2 a / db^2$ for the evolutionary outcome, and that a weakly decelerating trade-off is required at the singular point for evolutionary branching. Our focus in this study will be on the potential generation of diversity through branching, and the subsequent extinction of one of the strains.

For completeness we start with the case of a general linear trade-off

$$a = f(s) = AS + B. \tag{5}$$

Here (4) simplifies to give a PIP on which, aside from $s' = s$, we have another branch

$$s = 6 / (2B - 3A - 2). \tag{6}$$

This is a vertical straight line and obviously there are no closed regions on the PIP. For a numerical example we take $a = f(s) = 0.2273s + 2.09091$ which gives the vertical branch at $s = 4$. The PIP is as in figure 1(a) where we use a range of s between 3 and 5 (here the resident has positive densities and is stable and the trade-off has positive gradient). We use this range of s for subsequent figures. The PIP in figure 1 shows that there is an evolutionary singularity at $s = 4$ which is marginally evolutionarily stable (ES) and is

convergent stable (CS). This is in accord with routine adaptive dynamics analysis (Geritz et al., 1998) which locates the singularity via $\partial s / \partial s' \big|_{s=s'} = 0$ (which has the solution $s = 4$ here) and characterises it as ES if at the singularity $\partial^2 s / \partial s'^2 \big|_{s=s'} < 0$ (the value is 0 here) and as CS if at the singularity $\frac{\partial^2 s}{\partial b'^2} \bigg|_{b'=b} + \frac{\partial^2 s}{\partial b \partial b} \bigg|_{b'=b} < 0$ (which applies here). A simulation for the case of the linear trade-off is shown in the figure 1(b) and shows the expected attractor at $s = 4$.

We now turn to the case of a general quadratic trade-off

$$a = f(s) = AS^2 + BS + C. \quad (7)$$

Here (4) simplifies to give

$$3(s - s')(3As^2 + 2As^2s' + s(2 + 3B - 2C) + 3Ass' + 6) = 0. \quad (8)$$

On the PIP aside from $s = s'$ we have another branch

$$s' = -(3As^2 + s(2 + 3B - 2C) + 6) / (As(2s + 3)). \quad (9)$$

For any value of s this gives a unique value of s' and so this branch gives rise to no closed regions of either invadability or mutual invadability. However, we can have an open region on which a strain could in principle be lost on crossing the boundary (9). Since there are limits on the feasible range of s , there will also be other 'absorbing' boundaries corresponding to the extreme values of this parameter. From (3) we see that near the origin the fitness varies as $6(s' - s)/s$ and so non-invadability is the case below $s' = s$. Now (9) is continuous for positive s and hence the lowest of any pair of (positive) singularities must be attracting and the candidate to be branching. This is illustrated in our numerical example $a = f(s) = 0.0057s^2 + 0.1818s + 2.1818$ which displays generic features. The PIP is shown in figure 2(a) and highlights a singularity at $s = 4$ which is not ES but is CS (there is another singularity near $s = 8.5$ which is not ES or CS, see figure 4 later). The singularity at $s = 4$ is a branching point; thus quadratic trade-offs can certainly

lead to diversity. A simulation is presented in the figure and this shows the expected branching point; after branching the two strains diverge and respectively tend to the lower and upper feasible values of s . As shown, the orbit does not cross the boundaries on the TEP in figure 2(b) – which has the region of coexistence in grey – but approaches the top left corner. This is guaranteed by the lack of nullclines in the co-existence region. Such nullclines can only intersect the boundary of coexistence at specific points on the TEP, namely vertically above/below singular points or where the boundary of the coexistence region is vertical (Geritz et al. 1999). The coexistence region has no such points in the quadratic case, no nullclines appear and selection is uni-directional within the coexistence region. Inasmuch as this behaviour is generic (and there is a caveat here, we have only numerical studies in evidence) we conclude that quadratic as well as linear trade-offs do not display the behaviour we seek; diversity can evolve but not its subsequent loss.

For the cubic case we consider the following trade-off

$$a = f(s) = As^3 + Bs^2 + Cs + D \quad (10)$$

The fitness is now zero (using 4) when $s' = s$ and

$$As(2s + 3)s'^2 + s(2As^2 + (3A + 2B)s + 3B)s' + 3As^3 + 3Bs^2 + (3C - 2D + 2)s + 6 = 0 \quad (11)$$

Now on the PIP, aside from $s = s'$, we have another two branches which are the solutions of the above quadratic equation for s' . We can write the solutions in the form

$$s' = \frac{-t(s) \pm \sqrt{d(s)}}{k(s)} \quad (12)$$

with the obvious identifications of the smooth functions t, d, k . When $d(s) > 0$, this gives rise to two simultaneous branches on the PIP equally spaced above and below $s' = -t(s)/k(s)$. As s approaches a point where $d(s) = 0$ these branches join each other continuously with vertical gradient. Generically, further change in s takes us into an interval of s for which $d(s) < 0$ and here the only branch on the PIP is $s = s'$. If we allow

s to change in the opposite direction, then we either approach another point where $d(s) = 0$ or reach the end of the feasible range of s . In the first case we have a closed region on the PIP; in the second there is a closed region with a boundary which cannot be crossed. The above assumes $k(s) \neq 0$; if this is not so, asymptotes may modify the picture a little but generically we effectively still have closed regions. (If d, k vanish simultaneously, then the two branches are absent one side of the asymptote.) In summary the cubic case gives rise to closed regions on the PIP and the possibility of the loss of strain coexistence.

For a numerical example we take

$$a = f(s) = -0.06723484848s^3 + 0.8125s^2 - 3.045454546s + 6.484848483 \quad (13)$$

(We note that the high precision given here is to ensure the singular point is at precisely $b = 4$. The precision can be relaxed and the key behaviours still occur). This gives in addition to $s = s'$ two branches which are solutions of the corresponding explicit form of (11) and the PIP is shown in figure 3a. This displays the type of closed region described above as well as regions where there is only the branch $s = s'$. The figure shows two evolutionary singularities and indicates that the lower is neither ES nor CS whilst the higher while not ES is CS. Applying the above adaptive dynamics techniques locates the singularities at $s = 3.879$ and $s = 4$ and verifies the ES/CS results. The singularity at $s = 4$ is a branching point; thus cubic trade-offs can lead to diversity and also its loss because of the closed region. A simulation for the cubic case is shown in the figure 3(c) which shows the expected branching point near $s = 4$ but in addition shows the loss of diversity with increasing time. The TEP showing the region of coexistence indicates the oval coexistence region and nullclines which now do appear within this region (figure 3(b)). The nullclines do not cross therefore there is no further singular point in the dimorphic system and evolutionary loss is inevitable. The subsequent loss of diversity is illustrated further by plotting the evolutionary trajectory on the TEP. The positioning of the nullclines is such that once the trajectory reaches the boundary of coexistence the strain with lower s is necessarily beyond the monomorphic repeller. As the boundary is crossed it can be seen in the PIP that the strain with the lower (higher) value of s has positive (negative) fitness, meaning that it is the lower strain that will survive the extinction. Since this strain is necessarily beyond the repeller it will not be attracted back to the branching point but be

selected to ever lower beta values until the minimum bound of the trade-off is reached, as seen in the simulation (figure 3(c)). In this case, therefore, the host has reached a state of maximum defence. For cubic trade-offs (and quartic trade-offs, see later) we have performed numerical investigations that indicate that whenever we have a branching point, and the bounds of evolution are such that a 'full' oval exists on the PIP, then we see the behavior described. We can also demonstrate analytically that up to and including cubic trade-offs there can be no 'internal' singular point.

What perspective can be cast on our results by considering a trade-off of general degree n ? Equation (4) has now a (combined) degree in b, b' of $n+2$. Thus, with this trade-off invoked, after the factor $b - b'$ has been removed (4) yields

$$3(s - s')P(s, s') = 0 \tag{14}$$

where P has degree $n+1$. Concentrating on the second factor gives us a plane algebraic curve of this degree. Such curves consist of a finite number of smooth monotone segments which in either direction have endpoints which have horizontal or vertical tangents or are mathematical singularities (such as cusps, double points or isolated points); additionally segments may be unbounded (see figure 4, and below). Ovals can occur as a result of this structure. The evolutionary singularities of interest here are double points of the plane curve obtained by adding $b' = b$. The equation $P(b, b) = 0$ locating them yields a maximum number of $n+1$ (alternating attracting/repelling) evolutionary singular points. Regarded as a polynomial in b' , P has, from (4), degree $n-1$ which is therefore the maximum number of simultaneous branches on the PIP additional to $b' = b$.

The examples studied above conform to this behaviour as is illustrated in figure 4 which shows only zero contours of the fitness but uses a broader (often unfeasible) range of s . The linear case $n=1$ (not shown) is slightly anomalous since we might expect P to have degree 2 but, quite generally, it follows from (4) and (5) that the quadratic term in (14) vanishes and P is of degree 1 and a linear function of s alone. This means there is second vertical branch on the PIP and one singularity at the intersection of this branch and the branch $s' = s$ (see (6) above and the numerical example follow it). (Formally, these results still conform to our results on the maximum numbers of singularities and branches on the

PIP). In the quadratic example $n=2$ (figure 4a) we have two feasible singularities one repelling and one attracting (there is a third unfeasible one) and we see at most one PIP branch additional to $b'=b$. In the cubic example (figure 4b) we can now distinguish a second region contained between smoothly joining curves and their asymptote (the vertical axis) and a third region – with asymptote $b=-3/2$. There is again an attracting/repelling pair of feasible singularities (there are now two unfeasible singularities) and the maximum number (2) of simultaneous branches is certainly not exceeded. The cubic case illustrates the fact that the above general properties of plane algebraic curves allow for the existence of ovals on the PIP.

As a final illustration we consider a quartic trade-off, explicitly

$$a = f(s) = -0.01s^4 + 0.1007651515s^3 - 0.2434999998s^2 - 0.1014545467s + 3.412848488. \quad (15)$$

The PIP is shown in figure 5(a) and the results are similar to the cubic example. The figure again shows two evolutionary singularities and indicates that the lower is neither ES nor CS whilst the higher while not ES is CS. Applying the above adaptive dynamics techniques locates the singularities at $s = 3.8572$ and $s = 4$ and verifies the ES/CS results. The singularity at $s = 4$ is a branching point; thus quartic trade-offs can also lead to diversity and - because of the closed region - its loss. In figure 5(c) we show a simulation for the quartic case which shows the expected branching point near $s = 4$ and also loss of diversity. The trajectory after branching is also plotted on the TEP (figure 5(b)) which shows very similar behaviour to the cubic case discussed above. Again, there is no dimorphic singular point and when the coexistence boundary is crossed it is necessarily the lower strain, which is beyond the repeller, that survives. Again, therefore, the host population reaches a point of maximum defence. The final graph in figure 4 presents the result on a broader range. This agrees with the general results that there are a maximum of 5 evolutionary singular points (there are two complex ones here) and that the maximum number of simultaneous branches on the PIP is 3.

Discussion

Our results are concerned with the evolutionary loss of previously evolved diversity (explicitly dimorphism). We have studied this in the context of host resistance to micro-parasitism using a trade-off between increased defence in the host and reduced reproductive ability. By considering polynomial trade-offs of increasing degree we have seen that linear trade-offs cannot display the behaviour of interest; quadratic ones can give rise to dimorphism but this is unlikely to be lost in subsequent evolution; cubic and higher degree trade-offs can display branching leading to dimorphism and furthermore this may be subsequently lost. We have traced this behaviour to the occurrence of ovals in plane curves representing invasion boundaries on PIPs. Such ovals only appear when the curve is of sufficiently high degree and here this degree is related to that of the trade-off. Naively one might expect that more complex trade-off forms may lead to greater diversity since they may create a series of local niches (or more formally, attracting singular points) where multiple strains could coexist. In fact, we have shown the opposite to be true. It is natural to speculate that rather generally trade-offs of low 'complexity' might not lead to evolutionary loss of previously evolved diversity whereas those of higher complexity might well do so.

Previous studies have shown other examples of eco-evolutionary models that generate dimorphism through evolutionary branching followed by the evolutionary extinction of one strain as the population evolves outside of the region of coexistence (Kisdi, 1999; Kisdi et al., 2001; Dercole, 2003; Ammuset et al., 2014). The phenomenon of evolutionary extinction is therefore clearly not related to trade-off geometries alone but more deeply embedded in eco-evolutionary dynamics. However, for the most part in these examples the extinction occurs in such a way that the remaining strain is once again attracted towards the original evolutionary branching point, creating a branching-extinction cycle (Kisdi et al., 2001; Dercole, 2003; Johansson et al. 2010; Ammuset et al., 2014). In contrast, our results show that after the extinction the remaining strain has crossed an evolutionary repeller, and will instead move to a further attracting singular point or extremes of its trade-off. Kisdi (1999) showed similar behaviour to this in an asymmetric competition model for certain growth functions. We have shown that this behaviour is guaranteed by the shape that the 'oval' region of coexistence creates on the TEP.

The creation of a closed region on pairwise invasion plots (PIPs) and trait evolution plots (TEPs) requires the fitness function to be of sufficiently high degree. This may come as a result of, for example, an asymmetric competition term (Kisdi, 1999) where interactions are

dependent on trait values in a non-linear manner. Here we have shown that such closed regions can be easily generated through trade-offs of sufficiently high degree, namely 3rd order or higher. We may speculate that in general if the fitness function is of sufficiently high degree due to inherent non-linearities then not only branching to diversity but subsequent extinction is increasingly likely. We find this behaviour if we consider a different, non-polynomial but complex (sinusoidal), trade-off for our model system and if we consider a polynomial trade-off in a different model system (namely the predator-prey system considered in Bowers et al. 2003; see Appendix 2). We further note that the sinusoidal trade-off (Appendix 2) demonstrates a case where the remaining host evolves to minimum defence (high transmission) whereas the two cases in the main text saw the host evolve to maximum defence. Generically, the host may evolve to a maximum, minimum or a further attracting singular point depending on the number and ordering of singular points.

We have shown that if trade-offs are simply linear only monomorphic populations can ever exist, if they are non-linear of low-order (i.e. quadratic) then branching to dimorphism is possible, and if they are non-linear of high-order (cubic and above) then branching followed by extinction of one branch can occur. An important question is clearly how likely it is that trade-offs will be sufficiently complex in nature for our results to have relevance. It seems entirely possible that all evolutionary trade-offs, for example those arising through resource allocation or pleiotropy, are non-linear. However, experimental data is generally analysed purely to find the existence of trade-offs between life-history traits (Boots and Begon 1993, Kraaijeveld and Godfray 1997; and see Stearns 1992). Information about the shape of the trade-off is limited and often found by fitting data with linear models, or perhaps non-linear models of low degree (see Mealor and Boots 2006). However, it is perfectly reasonable to suppose that a highly non-linear trade-off function would fit the data just as well. As one example, from a mechanistic perspective, we might expect such complex trade-off shapes if defence (in our example here) is made up of multiple defence reactions as seen, for example, in *Drosophila melanogaster* which uses physical barriers as well as local and systemic immune responses to pathogens (Lemaitre & Hoffmann, 2007). Such complex trade-offs may be critical in determining the evolutionary behaviour of the system.

Acknowledgements

AB is supported by a Leverhulme Early Career Fellowship.

References

- Ammunét, T., Klemola, T. & Parvinen, K. (2014). Consequences of asymmetric competition between resident and invasive defoliators: a novel empirically based modelling approach. *Theor Popul Biol.* 92:107-17
- Boots, M. & Begon, M. (1993). Trade-offs with resistance to a granulosis virus in the Indian meal moth, examined by a laboratory evolution experiment. *Functional Ecology*, 7, 528-534.
- Boots, M., White, A., Best, A. & Bowers, R. (2014). How Specificity and Epidemiology Drive the Coevolution of Static Trait Diversity in Hosts and Parasites. *Evolution*.
- Bowers, R.G., Hoyle, A., White, A. & Boots, M. (2005). The geometric theory of adaptive evolution: trade-off and invasion plots. *J Theor Biol*, 233, 363-377.
- Bowers, R.G., White, A., Boots, M., Geritz, S.A.H. & Kisdi, E. (2003). Evolutionary branching/speciation: contrasting results from systems with explicit or emergent carrying capacities. *Evolutionary Ecology Research*. 5, 883-891.
- Bowers, R. G. (2011). On the determination of evolutionary outcomes directly from the population dynamics of the resident. *Journal of mathematical biology* 62, 901-924.
- de Mazancourt, C. & Dieckmann, U. (2004). Trade-off geometries and frequency-dependent selection. *Am. Nat.* 164, 765–778.
- Dercole, F. (2003). Remarks on branching-extinction evolutionary cycles. *J. Math. Biol.* 47, 569–580.
- Doebeli, M. & Dieckmann, U. (2000). Evolutionary branching and sympatric speciation caused by different types of ecological interactions. *Am. Nat.* 156, 77–101.
- Doebeli, M. & Ruxton, G.D. (1997). Evolution of dispersal rates in metapopulation models: Branching and cyclic dynamics in phenotype space. *Evolution* 51, 1730–1741.
- Geritz, S.A.H., Kisdi, E., Meszner, G. & Metz, J.A.J. (1998) Evolutionarily singular strategies and the adaptive growth and branching of the evolutionary tree. *Evolutionary Ecology* 12, 35–57.
- Geritz, S.A.H., van der Meijden, E. & Metz, J.A.J. (1999). Evolutionary dynamics of seed size and seedling competitive ability. *Theoretical Population Biology*, 55(3):324-343

- Hoyle, A., Bowers, R.G., White, A. & Boots, M. (2008). The influence of trade-off shape on evolutionary behaviour in classical ecological scenarios. *J Theor Biol*, 250(3), 498-511.
- Johansson, J., Ripa, J. & Kuckländer, N. (2010). The risk of competitive exclusion during evolutionary branching: effects of resource variability, correlation and autocorrelation. *Theor Popul Biol.* 2010 Mar;77(2):95-104.
- Kisdi, E., (1999). Evolutionary branching under asymmetric competition. *J. Theor Biol.* 197, 149–162.
- Kisdi, E., Jacobs, F.J.A. & Geritz, S.A.H. (2001) Red Queen evolution by cycles of evolutionary branching and extinction. *Selection* 2, 161–176.
- Koella, J.C. & Doebeli, M. (1999) Population dynamics and the evolution of virulence in epidemiological models with discrete host generations. *J. Theor. Biol.* 198, 461–475 .
- Lemaitre, B. and Hoffmann, J. (2007). The host defence of *Drosophila melanogaster*. *Annual Review of Immunology*, 25:697-743.
- Kraaijeveld, A. R. & Godfray, H. C. J. (1997) Trade-off between parasitoid resistance and larval competitive ability in *Drosophila melanogaster*. *Nature* 389, 278–280.
- Mealor, M.A. & Boots, M. (2006). An indirect approach to imply trade-off shapes: population level patterns in resistance suggest a decreasingly costly resistance mechanism in a model insect system. *J Evol Biol*, 19, 326-330
- Metz, J.A.J., Geritz, S.A.H., Meszéna, G., Jacobs, F.J.A. & van Heerwaarden, J.S. (1996). Stochastic and spatial structures of dynamical systems. In: van Strien, S.J., Verduyn Lunel, S.M. (Eds.), *KNAW Verhandelingen, Afd. Natuurkunde*. North Holland, Amsterdam, pp. 183–231.
- Roff, D.A. (2002). *Life History Evolution*. Sinauer Associates, Sunderland, MA.
- Rueffler, C., Van Dooren, T.J.M. & Metz, J.A.J. (2004). Adaptive walks on changing landscapes: Levin's approach. *Theor. Popul. Biol.* 65, 165–178.
- Stearns, S.C. (1992). *The Evolution of Life Histories*. Oxford: Oxford University Press.
- Van der Laan, J.D., Hogeweg, P. (1995). Predator-prey coevolution: Interactions across different timescales. *Proc. R. Soc. Lond. B* 259, 35–42.

Figures

Figure 1: (a) shows a PIP for the model represented by equations (1) with a linear trade-off in which $a = f(s) = 0.2273s + 2.09091$. Here invadable regions (positive fitness) are black and uninvadable regions (negative fitness) white. (b) shows a simulation of the adaptive dynamics process indicating that traits evolve towards the singular point at $s = 4$. The trade-off function is shown in the inset figure in (b). Other parameters are $b = 1$, $q = 1$, $r = 1$ and $x = 1$.

Figure 2: (a) shows a PIP for the model represented by equations (1) with a quadratic trade-off in which $a = f(s) = 0.0057s^2 + 0.1818s + 2.1818$. Here invadable regions (positive fitness) are black and uninvadable regions (negative fitness) white. (b) shows a TEP with the grey region indicating where two traits can coexist and with representative evolutionary trajectories. (c) shows a simulation of the adaptive dynamics process indicating that traits evolve towards the branching point at $s = 4$ and when nearby undergo disruptive selection to form a dimorphic population. The TEP and the simulations indicate that the dimorphic population will evolve to be composed of the minimum and maximum trait values. The trade-off function is shown in the inset figure in (c). Other parameters are $b = 1$, $q = 1$, $r = 1$ and $x = 1$.

Figure 3: (a) shows a PIP for the model represented by equations (1) with a cubic trade-off in which $a = f(s) = -0.06723484848s^3 + 0.8125s^2 - 3.045454546s + 6.484848483$. Here invadable regions (positive fitness) are black and uninvadable regions (negative fitness) white. (b) shows a TEP with the grey region indicating where two traits can coexist, isoclines represented by white lines and with representative evolutionary trajectories. (c) shows a simulation of the adaptive dynamics process indicating that traits evolve towards the branching point at $s = 4$ and when nearby undergo disruptive selection to form a dimorphic population. The TEP and the simulations indicate that the dimorphic population will evolve to trait values that cross the boundary of coexistence and here one trait becomes extinct. The trade-off function is shown in the inset figure in (c). Other parameters are $b = 1$, $q = 1$, $r = 1$ and $x = 1$.

Figure 4: Extended PIPs showing only zero contours of the fitness and using a broader (often unfeasible) range of s . (a) The quadratic example of figure 2. (b) The cubic example of figure 3. (c) The quartic example of figure 5. The diagrams show that in accord with general theory on this broad range, for a trade-off of degree n , there are a maximum of $n+1$ singularities and $n-1$ simultaneous PIP branches in addition to $b'=b$.

Figure 5: (a) shows a PIP for the model represented by equations (1) with a quartic trade-off in which

$$a = f(s) = -0.01s^4 + 0.1007651515s^3 - 0.2434999998s^2 - 0.1014545467s + 3.412848488.$$

Here invadable regions (positive fitness) are black and uninvadable regions (negative fitness) white. (b) shows a TEP with the grey region indicating where two traits can coexist, isoclines represented by white lines and with representative evolutionary trajectories. (c) shows a simulation of the adaptive dynamics process indicating that traits evolve towards the branching point at $s = 4$ and when nearby undergo disruptive selection to form a dimorphic population. The TEP and the simulations indicate that the dimorphic population will evolve to trait values that cross the boundary of coexistence and here one trait becomes extinct. The trade-off function is shown in the inset figure in (c). Other parameters are $b = 1$, $q = 1$, $r = 1$ and $x = 1$.

Appendix 1

Equation (1) yields an infected equilibrium, $(X, Y) = (X^*, Y^*)$ where

$$X^* = (r + b + x)/s \quad \text{and} \quad Y^* = \frac{(r + b + x)(as - bs - q(r + b + x))}{s(rs + bs + q(r + b + x))} \quad (\text{A1})$$

A proxy for the invasion fitness is obtained from the invasion dynamics

$$\begin{aligned} dX'/dt &= a'X' - qX'(X^* + Y^* + X' + Y') - bX' - s'X'(Y^* + Y') + xY' \\ dY'/dt &= s'X'(Y^* + Y') - (r + b + x)Y' \end{aligned} \quad (\text{A2})$$

via the Jacobian $J(0,0)$ obtained from $J(X', Y')$ by evaluation at $(X', Y') = (0,0)$. Only a and s vary between strains. The determinant of $J(0,0)$ yields for the fitness

$$s(b, b') = (a + b + g)(a' - q(X^* + Y^*) - b - b'Y^*) + g'Y^* \quad (\text{A3})$$

where the notation anticipates the introduction of a trade-off $a = f(s)$. In our case $q = b = x = r = 1$ we find

$$X^* = 3/s \quad \text{and} \quad Y^* = 3(as - s - 3)/(s(2s + 3)) \quad (\text{A4})$$

and

$$s(s, s') = 3a' - 9 \frac{(as + s)}{s(2s + 3)} - 3 - \frac{6s'(as - s - 3)}{s(2s + 3)}. \quad (\text{A5})$$

We can see that the perspective of this paper may well apply to a more general class of eco-evolutionary models. The dynamics of such models are often linear in parameters and of a particularly simple polynomial form in the densities which leads to the equilibria being rational functions of the parameters. The proxy for the fitness obtained from the invasion Jacobian is then polynomial in the parameters and equilibrium densities and hence rational in the parameters. This has the consequence that the invasion boundaries are polynomial in the parameters. Such a structure underlies the more explicit analysis of this paper and –

with polynomial trade-offs imposed – leads us in this more general setting to the consideration of invasion boundaries which are plane algebraic curves.

Appendix 2

We present figures from two more examples in this appendix. Firstly, we show plots for the host-parasite model of the main text using a sinusoidal trade-off, $a(b) = 3 + 0.5(b-4) - 0.0145\sin(p(b-4))$ in figure A1. This shows very similar behaviour to the higher degree polynomial trade-offs in figures 3 and 4 in the main text. This highlights that it is not polynomial trade-offs per se, but sufficiently ‘complex’ trade-offs, that result in evolutionary loss of diversity. (Parameter values and methods are as described in the main text).

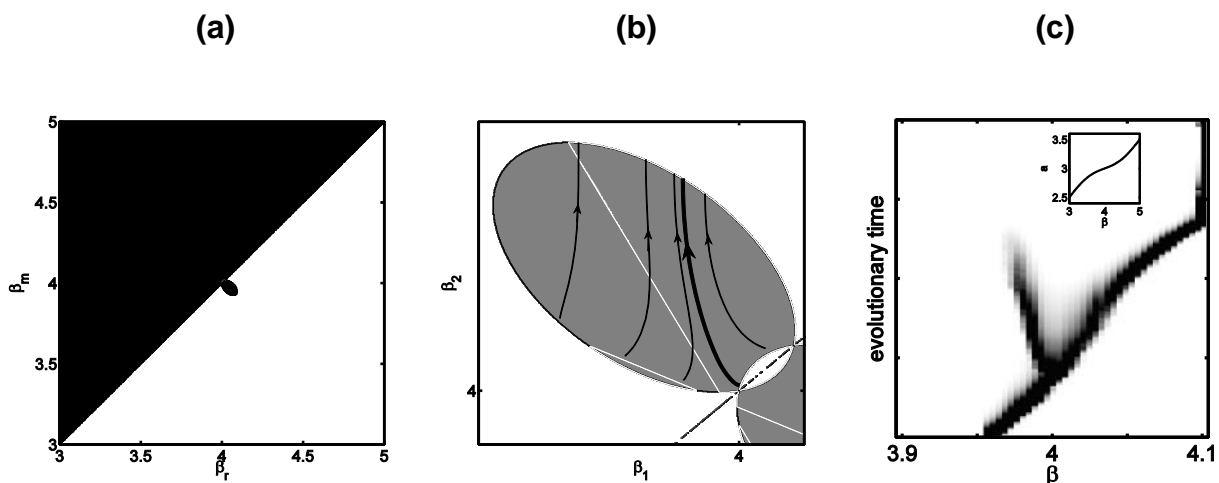


Figure A1: (a) shows a PIP for the model represented by equations (1) with a sinusoidal trade-off in which $a(b) = 3 + 0.5(b-4) - 0.0145\sin(p(b-4))$. Here invadable regions (positive fitness) are black and uninvadable regions (negative fitness) white. (b) shows a TEP with the grey region indicating where two traits can coexist and with representative evolutionary trajectories. (c) shows a simulation of the adaptive dynamics process indicating that traits evolve towards the branching point at $s = 4$ and when nearby undergo disruptive selection to form a dimorphic population. The TEP and the simulations indicate that the dimorphic population will evolve to trait values that cross the boundary of coexistence and here one trait becomes extinct. The trade-off function is shown in the inset figure in (c). Other parameters are $b = 1$, $q = 1$, $r = 1$ and $x = 1$.

We also present results from a predator-prey model to highlight that our results are more generally applicable. We take the predator-prey system from Bowers et al. (2003),

$$\begin{aligned}\frac{dN}{dt} &= N(r - hN - cP) \\ \frac{dP}{dt} &= P(ceN - d)\end{aligned}\tag{A5}$$

taking $h, e, d = 1$ and a cubic prey trade-off of $r(c) = -7.5c^3 + 22.75c^2 - 20.4c + 8.75$. This produces the plots shown in figure A2, which looks very similar to the results from the cubic host-parasite model, in particular showing evolutionary loss of diversity.

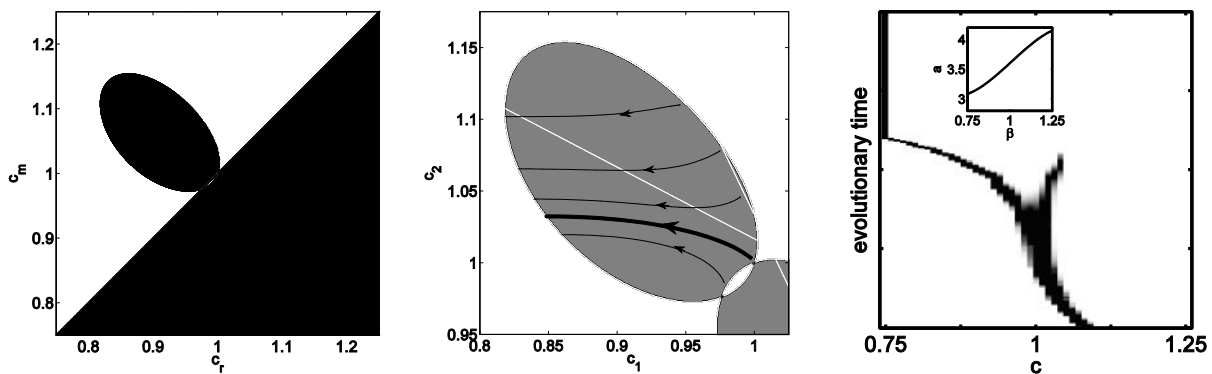


Figure A2: (a) shows a PIP for the predator-prey model represented by equations (A6) with a cubic trade-off in which $r(c) = -7.5c^3 + 22.75c^2 - 20.4c + 8.75$. Here invadable regions (positive fitness) are black and uninvadable regions (negative fitness) white. (b) shows a TEP with the grey region indicating where two traits can coexist and with representative evolutionary trajectories. (c) shows a simulation of the adaptive dynamics process indicating that traits evolve towards the branching point at $c = 1$ and when nearby undergo disruptive selection to form a dimorphic population. The TEP and the simulations indicate that the dimorphic population will evolve to that cross the boundary of coexistence and here one trait becomes extinct. The trade-off function is shown in the inset figure in (c). Other parameters are $d = 1$, $e = 1$ and $h = 1$.